Journal of
Polymer Materials

Tech Science Press

Doi:10.32604/jpm.2026.074431

ARTICLE

Rapid-Curing, Precision-Sprayable Polyoxytetramethylene Glycol Based Polyurethane-Urea Coatings with High Mechanical Performance

Zhipeng Ran*, Peishuang Xiao, Shuen Liang, Keping Chen and Xiuli Zhao*

Institute of Chemical Materials, China Academy of Engineering Physics, Mianyang, 621900, China

*Corresponding Authors: Zhipeng Ran. Email: ranzp@caep.cn; Xiuli Zhao. Email: zhaoxiuli@caep.cn

Received: 11 October 2025; Accepted: 30 December 2025; Published: 03 April 2026

ABSTRACT: This study presents the development of high-performance, solvent-free polyurethane-urea (PU) elastomeric coatings engineered for rapid curing and precise sprayability. Utilizing polyoxytetramethylene glycol (PTMG) as the primary polyol and a static-mixing spraying technique, the formulations were systematically optimized. It was found that a soft-segment content of 64% yields optimal mechanical properties, achieving a remarkable tensile strength exceeding 30 MPa. Crucially, the incorporation of an ultra-low concentration (0.002 wt%) of dibutyltin dilaurate catalyst was sufficient to enhance curing completeness and mechanical performance while effectively eliminating moisture-induced foaming, a common challenge in solvent-free spray applications. The gel and tack-free times were successfully reduced to the order of minutes through strategic formulation with the chain extender dimethylsulfide-toluene diamine, minimizing reliance on high catalyst loadings. The resultant PTMG-based coatings exhibit exceptional comprehensive properties, including a tensile strength >30 MPa, elongation at break >400%, and a tear strength of 66 N/mm, significantly surpassing conventional polypropylene-diamine-based polyurea systems. Furthermore, the coatings demonstrated superior low-temperature flexibility, evidenced by a glass transition temperature of −53°C, and suppressed soft-segment crystallinity. The solvent-free nature and tunable curing kinetics of this system enable precise spraying on complex geometries, effectively overcoming thickness-control limitations for small-object applications. This work establishes a sustainable and high-performance coating solution ideal for demanding impact- and corrosion-resistant protective layers.

KEYWORDS: Polyurethane-urea; coatings; mechanical performance; solvent-free

1 Introduction

Spray polyurea (PUA) elastomer is a high-performance material developed from polyurethane, and exhibits unique properties such as rapid curing without any solvent, insensitivity to humidity, exceptional physical properties such as high hardness, flexibility, tear strength, tensile strength, chemical and water resistance [1–3]. Due to the aforementioned specific performance, spray PUA elastomeric coatings have attracted great interest in various fields, such as corrosion protection [4], impact resistance [5–7], and building protection [8], and anti-fouling [9]. Amine-terminated polyoxypropylene diamine is one of the most important components for polyurea, and the curing reaction between polyether diamine and isocyanate is as fast as several seconds [10–12]. Because of the above fast-curing properties, a special two-component airless sprayer is usually essential to prepare PUA, which delivers two components to the spray gun in a specific ratio and mixes the two components homogeneously by quick head-on collision [13]. The equipment

has a high output rate of 1 to 20 kg per minute, making it ideal for efficiently spraying buildings, reservoirs, and other large-scale engineering projects [14].

However, there is also significant demand for applying spray elastomeric coatings to smaller objects. But the large output quantity of PUA derived from polyoxypropylene diamine suffers from difficult control of coating thickness and spray area for small objects, which results in great wastes of raw materials and extremely uneven coating thickness for complicated shapes of small objects [15,16]. In addition, some specific application areas, such as anti-impact protection and anti-blast shield, have a pressing demand for excellent mechanical strength and elongation for elastomers. Usually, the tensile strength and elongation of polyoxypropylene diamine-based PUA are 10~20 MPa and 300%~500%, respectively [6], which may be insufficient for the above specific applications.

It has been widely reported that poly (tetramethylene ether glycol) (PTMG) based polyurethane elastomer is much stronger in mechanics than polyoxypropylene [17–19]. The curing rate of hydroxy-terminated PTMG with isocyanate is much gentler than amine-terminated polyoxypropylene diamine, and is able to be adjusted by the content of the catalyst. Due to the lower curing rate, the PTMG-based polyurethane is likely able to be sprayed by traditional premix methods with an adjustable output flow rate. Therefore, PTMG seems to have greater potential for the above applications of high performance and smaller objects. However, different from other applications of PU such as casting, injection molding and adhesive, spray of polyurethane suffers from the dramatic effect of moisture in the atmosphere [20,21]. The moisture could react with -NCO to produce CO_2, and further lead to foaming and degradation of the mechanical strength of polyurethane elastomeric coatings [22]. Therefore, it is still a huge challenge to prepare elastomeric coatings based on hydroxy-terminated PTMG with high mechanical performance.

In this work, PTMG and diphenylmethane diisocyanate (MDI) are used to prepare solvent-free polyurethane-urea (PU) elastomeric spray coatings. The content of the catalyst is carefully adjusted to prevent PU coatings from moisture-induced foaming. Effects of soft-segment (SS) content, catalyst content, polyether molecular weight and polyether type on processing properties, mechanical performance, morphology, density and thermal properties of coatings are studied. Finally, solvent-free coatings with tensile strength above 30 MPa and 400% elongation at break are acquired.

2 Experimental Section

2.1 Materials

PTMG with a molecular weight of 1000 g/mol (PTMG1000) and 2000 g/mol (PTMG2000), and polyoxypropylene diamine with molecular weight of 2000 g/mol (D2000) were acquired from Shandong Haoshun Chemical Industry Co., Ltd., Jinan, Shandong Province, China. The hydroxyl value of PTMG1000 and PTMG2000 are 111.2 mg KOH/gand 56.1 mg KOH/g, respectively. Dimethylsulfide-toluene diamine (DMTDA) and dibutyltin dilaurate (DB) were obtained from Sinopharm Group Chemical Reagent Co., Ltd., Shanghai, China both with a purity of 95%. DMTDA and DB were used as a chain extender and catalyst, respectively. MDI specified as MDI50 and Carbonized diimide modified MDI (CMDI) were purchased from Wanhua Industrial Group, Yantai, Shandong Province, China. The chemical structures of these materials are shown in Scheme 1.

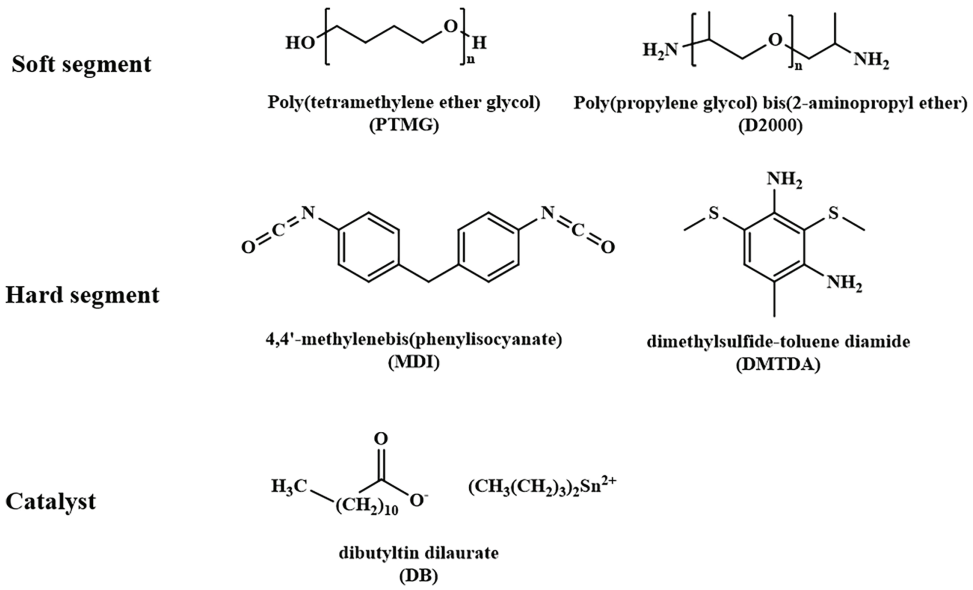

Scheme 1: Chemical structures of materials

2.2 Synthesis of Component A and Component B

125 g PTMG2000 was placed into a three-necked flask, and was heated to 120°C. After PTMG2000 was melted, the flask was vacuumed for two hours to remove the trace water in PTMG2000. Next, the temperature of the flask was reduced to 60°C, and a calculated amount of MDI was put into the flask. Component A with a -NCO% value of 13.9% was acquired after a two-hour reaction and denoted as MDI-2000. MDI-1000, CMDI-2000 and CMDI-1000 were also prepared by the above method. The composition of Component A is shown in Table 1. Component B was obtained by directly mixing PTMG, DMTDA and the catalyst according to the calculated proportion. The ratio (R) of -NCO value of Component A to the sum of -OH and -NH_2 in Component B was controlled to 1.10.

Table 1: Formulations of component A

Code	MDI, g	CMDI, g	PTMG1000, g	PTMG2000, g
MDI-1000	125	/	109	/
MDI-2000	125	/	/	135
CMDI-1000	/	125	85	/
CMDI-2000	/	125	/	105

PU coatings with a series of SS contents were prepared by adjusting the PTMG content in Component A and Component B. For example, 48.1 g MDI and 51.9 g PTMG2000 were used to synthesize component A, and 76.3 g PTMG2000 and 23.7 g DMTDA were used to prepare Component B. The coating with a SS content of 64% (PU2-S64) was derived from the above Component A and Component B. PU2-S80, PU2-S71, PU2-S53 and PU2-S41 were also prepared according to the above method (Table 2). The SS comprises the PTMG from Component A and the PTMG from Component B, while the hard segment included MDI and DMTDA. The SS content was defined as the percentage of PTMG in the formulation, which is calculated as the mass of PTMG divided by the total mass of PTMG, MDI, and DMTDA.

Table 2: Formulations of PU coatings with a series of SS contents

Code	Component A		Component B			
	MDI, g	PTMG2000, g	PTMG2000, g	DMTDA, g	R	SS, %
PU2-S80	31.6	68.4	92.5	7.5	1.10	80
PU2-S71	41.0	59.0	83.3	16.7	1.10	71
PU2-S64	48.1	51.9	76.3	23.7	1.10	64
PU2-S53	59.5	40.5	65.0	35.0	1.10	53
PU2-S41	71.4	28.6	53.1	46.9	1.10	41

PU2-S64 was chosen to investigate the effect of catalyst concentration on coating properties. 0.0025%, 0.005%, 0.01%, 0.05%, and 0.25% DB were added into Component B of PU2-S64 to prepare PU coatings with a series of catalyst concentrations and the coatings were denoted as PU2-C0.0025, PU2-C0.005, PU2-C0.01, PU2-C0.05 and PU2-C0.25, respectively. The formulation PU2-S64 did not contain a catalyst; therefore, it was equivalent to PU2-C0.

PTMG1000, D2000 and PTMG2000 were used to prepare PU coatings with a series of polyether polyol types. The formulation with 0.0025% DB added to PU2-S64 was designated as PU2-S64C, which subsequently served as the baseline formulation. In this formulation, D2000 was used to replace PTMG2000 in Component B to study the impact of D2000 on coating performance. Based on the increasing content of D2000, the coating samples were labeled as PU2-S64C-D1, PU2-S64C-D2, and PU2-S64C-D3, respectively. The specific composition of Component B is provided in Table 3. Additionally, we prepared PU1-S64C using MDI-1000 as Component A instead of that of MDI-2000 to study the influence of Component A. The -NCO% value of Component A was kept at 13.9%, and the coatings were prepared by the formulations shown in Table 3.

Table 3: Formulations of PU coatings with a series of polyether polyol types

Code	Component A	Component B			
		PTMG2000, g	D2000, g	DMTDA, g	DB, %
PU1-S64C	MDI-1000	76.3	/	23.7	0.0025
PU2-S64C	MDI-2000	76.3	/	23.7	0.0025
PU2-S64C-D1	MDI-2000	40.5	35.8	23.7	0.0025
PU2-S64C-D2	MDI-2000	20.3	56	23.7	0.0025
PU2-S64C-D3	MDI-2000	/	76.3	23.7	0.0025

2.3 Spray of PU

Coatings were spray-coated onto aluminum plates using an UNIKIS750 in a spray booth. The spray gun utilized compressed air at 0.5 MPa to atomize the coating into droplets. The spray distance was maintained at approximately 20–30 cm, with a traversing speed of about 20 cm/s. The flow rate of the coating material was controlled at around 30 mL/min. The ratio of Component A to Component B was 1:1 by volume. The relative humidity and temperature during spray and subsequent curing processes were adjusted to 70%~90% RH and 18°C~25°CRH, respectively. The PU coatings were sprayed to a thickness of approximately 1 mm and cured for 7 days at room temperature for performance tests.

2.4 Characterization

Tensile tests were conducted according to GB/T528-1998, and coatings were cut into type 2A for tests. Tear properties were carried out according to the unnicked angle tear strength of GB/T529-1999. The coating was sheared to a size of about 2 cm × 1 cm × 1 mm for the density test. At least 5 pieces of sheared samples were needed for each coating. The samples were weighed and measured to obtain weight and volume. Density was calculated by averaging the ratio of weight to volume for each piece. The differential thermal scanning analysis (DSC) test was processed from −70°C to 120°C a heating rate (β) of 20 K/min with a TA calorimeter model DSC-Q100 (TA Instruments, Inc., Shanghai, China) using nitrogen (caudal of 50 mL/min) as purge gas. 1 to 5 mg samples were sealed in aluminum pans. A sealed empty pan was used as the reference. And the temperature of samples was maintained at −70°C for 5 min before test. The dynamic mechanical analysis (DMA) was measured on a DMA Q800 (TA Instruments, Inc., Shanghai, China) at a frequency of 2 Hz with amplitude at 0.02 mm. The sample was maintained at −120°C for 10 min and then heated at a rate of 2°C/min. Rectangular bars of 10 mm × 5 mm × 1 mm were used as specimens for bend testing. Scanning electron microscopy images were obtained on a LEO 1530 FESEM (Carl Zeiss AG, Shanghai, China) to survey the cross-sections of the coatings. The coating thickness was measured using the eddy current mode of the Minitest600 coating thickness gauge. The specific measurement method was as follows: the coating was sprayed onto a flat aluminum alloy substrate, and the thickness was measured at least 10 times using a Minitest600 (EPK Instruments GmbH, Qingdao, Shandong Province, China) coating thickness gauge, with the average value taken as the coating thickness. Fourier-transform infrared spectroscopy (FTIR, Tensor 27 spectrometer, Bruker Corporation, Shanghai, China) was carried out in attenuated total reflectance mode with scanning range from 4000 to 650 cm^{-1}. The viscosity was measured using a Brookfield DV3THB viscometer (Brookfield Engineering Laboratories, Inc., Shanghai, China) with a No. 52 rotor. The system was set to the target temperature and allowed to equilibrate for 15 min after rotor installation. The gap between the rotor and the plate was then adjusted to 0.001 inch. Following sample loading, the system was maintained at the set temperature for another 15 min. During measurement, the rotational speed was adjusted to maintain the torque between 20% and 80%.

3 Results and Discussion

3.1 Preparation of PU Coatings

Spray PU or PUA elastomeric coatings are usually used as a high-build coating for various applications, which requires a fast cure rate and solvent-free formulation in order to spray with high efficiency [14]. The two-component airless sprayer based on head-on collision mixing is a widely used technology, but suffers from overlarge output flow rate and viscosity constraints of components.

In current studies, a series of solvent-free and fast-curing PU coatings are prepared by air spraying based on static mixing (Fig. 1a). 134 μm thick coatings with a width as small as 4 cm could be obtained by this method (Fig. 1b, the coating thickness of the samples ranged from 83.1 to 194.5 μm, with an average value of 134.3 μm), which is very different for head-on collision mixing-based airless sprayer. A cylinder Φ28 cm × 12 cm in size is coated with PU elastomer by spraying, and it is very uniform in terms of the coating thickness (Fig. 1c). These results show that the static mixing-based air spraying is suitable for coating of small objects, as a result of adjustable output flow rates for a wide range.

The viscosity of components, particularly component A, is one of the most important parameters for the above spray technology. MDI and CMDI are used as isocyanates to construct Component A of the coating. The effect of isocyanate type and molecular weight of PTMG on the viscosity of Component A has been shown in Fig. 2. The viscosity of CMDI-based Component A is approximately twice as high as that of

MDI-based Component A, which implies MDI is more appropriate to synthesize component A. Although PTMG2000 has a greater viscosity than PTMG1000, the viscosity of MDI-2000 is approximately equal to that of MDI-1000. The viscosity of MDI-2000 decreases from 5.5 to 0.55 Pa·s with temperature increasing from 15°C to 55°C, and the Component A is suitable for spray coating applicationat room temperature.

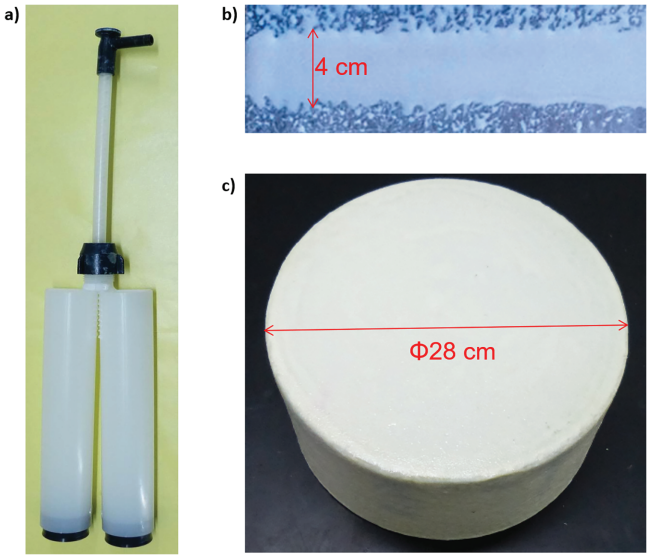

Figure 1: (**a**) a photograph of the air sprayer based on static mixing, (**b**) several lines of the coating created by separate one-off spray, (**c**) a Φ28 cm × 12 cm cylinder coated with PU elastomer by spraying method

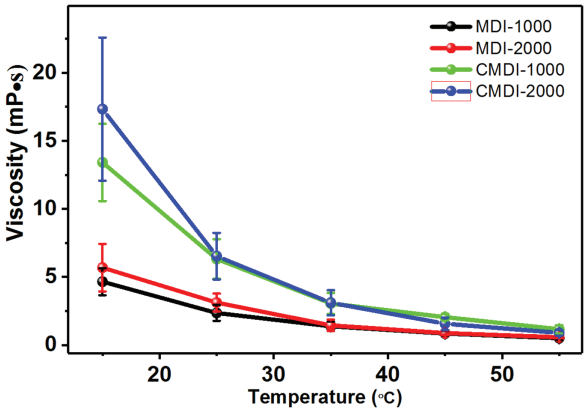

Figure 2: Viscosity of component a derived from MDI and CMDI

3.2 Effect of SS Content

In PU materials, the SS content has a dramatic effect on mechanical and thermal properties [17]. So, PU coatings with a series of SS contents were prepared, and processing properties, mechanical performance, and thermal performance were studied systematically.

The SS content was adjusted from 80% to 41%, and the coatings changed from soft to hard as SS content decreased (Fig. 3a). Tensile tests indicate that the coatings show a large elongation, and the elongation decreases from 650% to 200% as SS content is reduced from 80% to 41% (Figs. 3b and 4a). The tensile strength of PU2-S80, PU2-S71, PU2-S64 and PU2-S53 is 8.1, 14.5, 21.9 and 12.9 MPa, respectively, and PU2-S64 shows

the maximal tensile strength (Fig. 4a). The tensile modulus of PU2-S80, PU2-S71, PU2-S64, and PU2-S53 are 5.8, 29.6, 47.0, and 115.0 MPa, respectively. The modulus decreases with decreasing SS content. The toughness values for PU2-S80, PU2-S71, PU2-S64, and PU2-S53 are 20.8, 42.9, 37.2, and 21.7 MJ/m^3, respectively. The toughness initially increases and then decreases as the SS content is reduced, reaching a maximum at a ss content of 71%. The tear strength of PU2-S80, PU2-S71, PU2-S64 and PU2-S53 are 29, 53, 66 and 77 N/mm, respectively, and increase with the decrease in SS content (Fig. 4b). PU2-S41 is too fragile to be cut into specimens for tensile and tear tests, and the corresponding strength is unavailable. Gel time of PU2-S80, PU2-S71, PU2-S64, PU2-S53 and PU2-S41 are 24, 7, 2.8, 1.8 and 0.5 min, respectively, and the corresponding tack-free time are 1 day, 2 h, 17, 14 and 2 min, respectively (Fig. 4c). Fig. 4c demonstrates the gel time and tack-free time dramatically depend on the ratio of DMTDA to MDI. Density of coatings is 0.95, 1.00, 1.03, 1.05 and 1.08 g/cm^3 for PU2-S80, PU2-S71, PU2-S64, PU2-S53 and PU2-S41, respectively, and the increase of the ratio of DMTDA to MDI results in increase of the density (Fig. 4d).

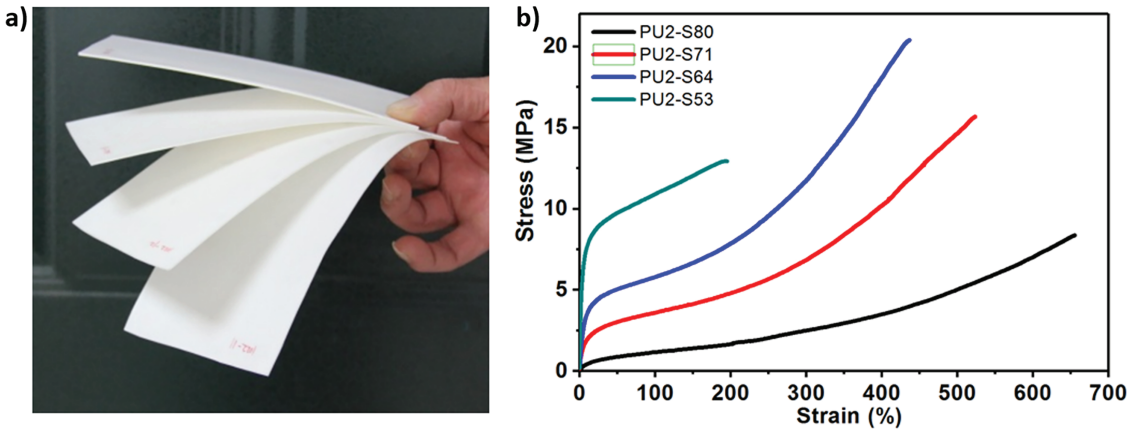

Figure 3: PU coatings with a series of content of SS. (**a**) a digital photo and (**b**) curves of tensile stress vs. strain

The results indicate that a SS content of 64% optimizes mechanical properties. DMTDA is an amine-based chain extender, and the reaction rate between amine and MDI is much larger than that of the hydroxy groups of PTMG and MDI. As a result of faster reaction rate, DMTDA dominates the gel time and tack-free time to a large extent. The decrease in coating density is mainly caused by carbon dioxide gas from the reaction between moisture in the atmosphere and -NCO. So, lower DMTDA concentration leads to longer gel time, and further results in the decrease in coating density.

DSC was used to investigate the glass transition and SS crystallization process of the PU coatings (Fig. 5). It is obvious that PU2-S80 shows a glass transition point (Tg) at −59.8°C and a SS crystallization process at 16.1°C and 36.4°C (Fig. 5a). The effect of SS content on Tg is negligible in DSC data, and the PU coatings with different SS content show an approximate Tg value of −60°C. The SS crystallization enthalpies of PU2-S80, PU2-S71, PU2-S64, PU2-S53, and PU2-S41 are determined to be 15.59, 7.78, 3.51, 1.47, and 0.83 J/g, respectively (Fig. 5b). The crystallization enthalpy decreases with the reduction in SS content, and the reduction in crystallization enthalpy is markedly more rapid than the decrease in SS content. This indicates that the presence of hard segments significantly restricts the crystallization behavior of the SS.

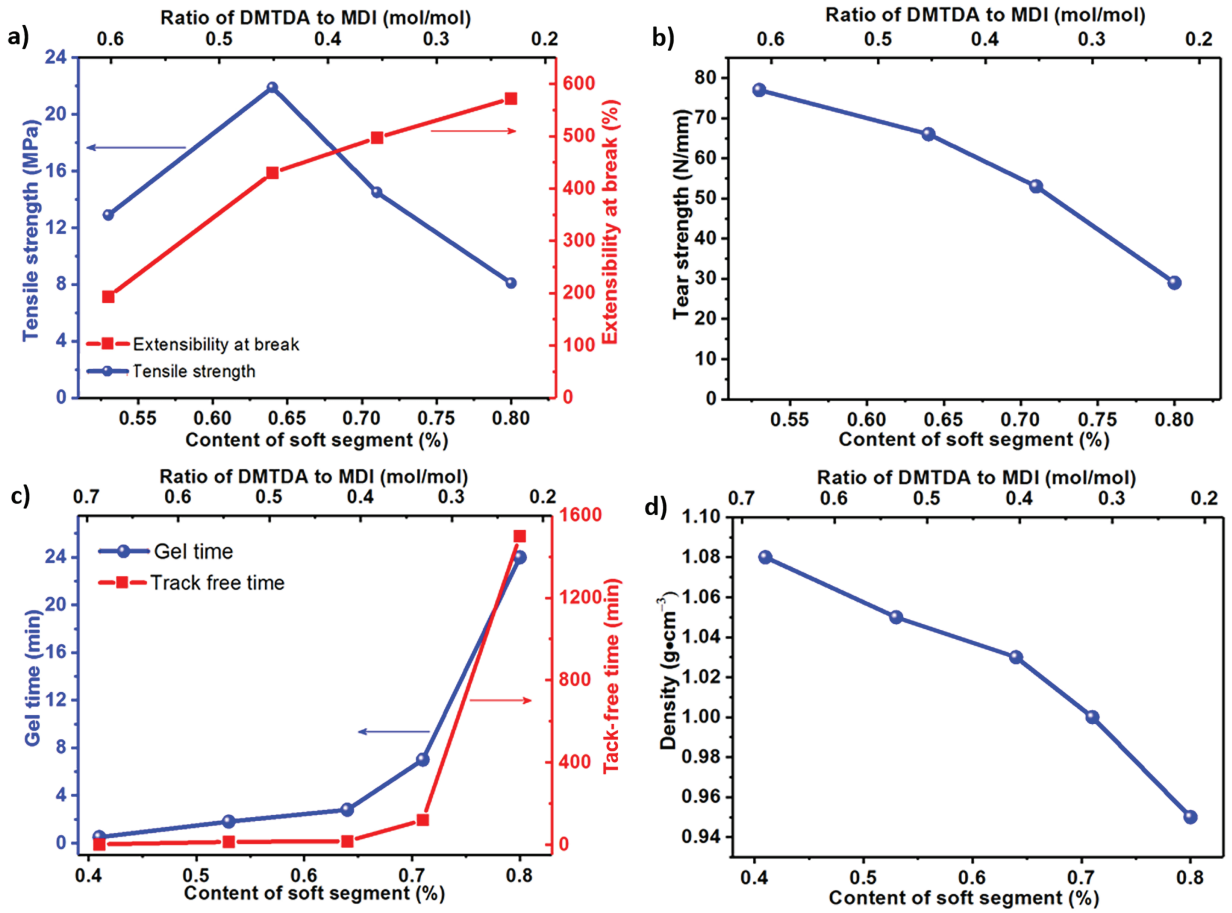

Figure 4: Effect of SS content on (**a**) tensile strength and extensibility at break, (**b**) tear strength, (**c**) gel time and tack-free time and (**d**) density of coatings

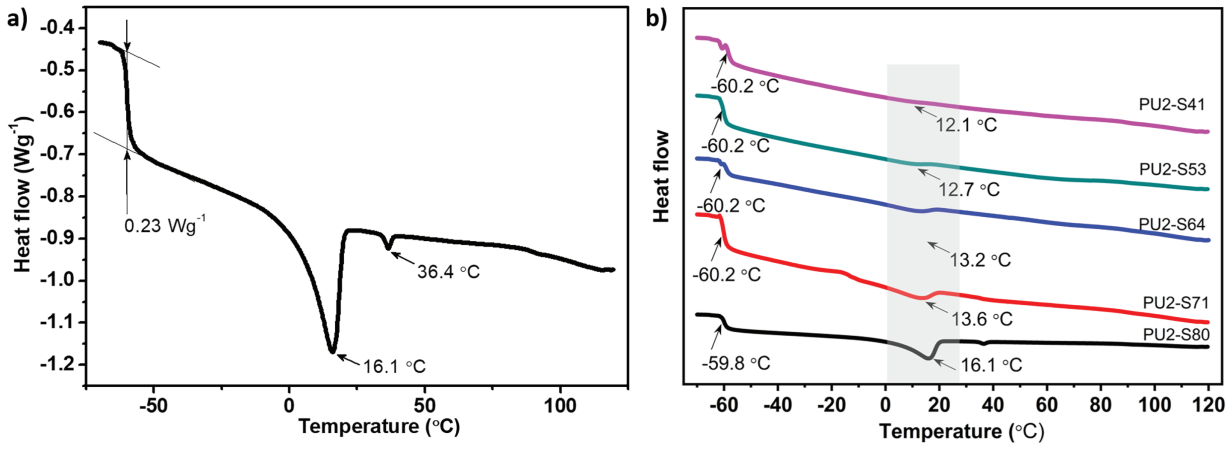

Figure 5: (**a**) the DSC curve of PU2-S80, (**b**) effect of SS content on temperature of glass transition point and SS crystallization. The crystalline peak of PTMG is indicated by the gray shaded area

The dynamic mechanical performances of the coatings are evaluated by DMA (Fig. 6). Regarding the storage modulus of the PU coatings, as shown in Fig. 6a, the values for PU2-S80, PU2-S71, PU2-S64, PU2-S53, and PU2-S41 increase progressively within the temperature range from −40°C to 150°C. A lower SS content implies a higher hard-segment content. Above the glass transition temperature (Tg), the hard segments act as physical cross-links, resulting in an increase in the modulus of the coatings as the SS content decreases. However, below −80°C, the storage modulus of PU2-S80 increases significantly. Although PU2-S80 has the lowest hard-segment content, DSC data indicates that its SS possesses the highest degree of crystallinity. In this low-temperature region, the SS has already crystallized, causing the storage modulus to be influenced by both the SS crystallinity and the molecular chain structure. As for the loss modulus, the values for PU2-S80, PU2-S71, PU2-S64, PU2-S53, and PU2-S41 decrease sequentially with the reduction in SS content (Fig. 6b). This suggests that the hard segments are the primary contributors to the increased internal friction within the coating. Furthermore, the Tg, identified from the peak of the loss modulus curve, exhibits a slight shift from −59°C to −67°C as the SS content decreases. The Tg values obtained from DSC studies differ from those determined by DMA, which can be attributed to the different properties measured by each technique—specifically, the change in specific heat capacity in DSC and that in mechanical properties in DMA. The loss factor (tan δ) curve displays a distinct peak at approximately −53.5°C for the PU coatings upon heating, which is attributed to the glass transition (Fig. 6c). Notably, PU2-S80 exhibits two additional tan δ peaks at 4.3°C and 33.6°C, which are associated with the crystallization of the SS. Regarding the shape of the tan δ curve, the absence of a single peak and the very slow decay of tan δ above the Tg indicate that the coatings are not ideal rubber-like elastomers but rather complex multi-phase systems.

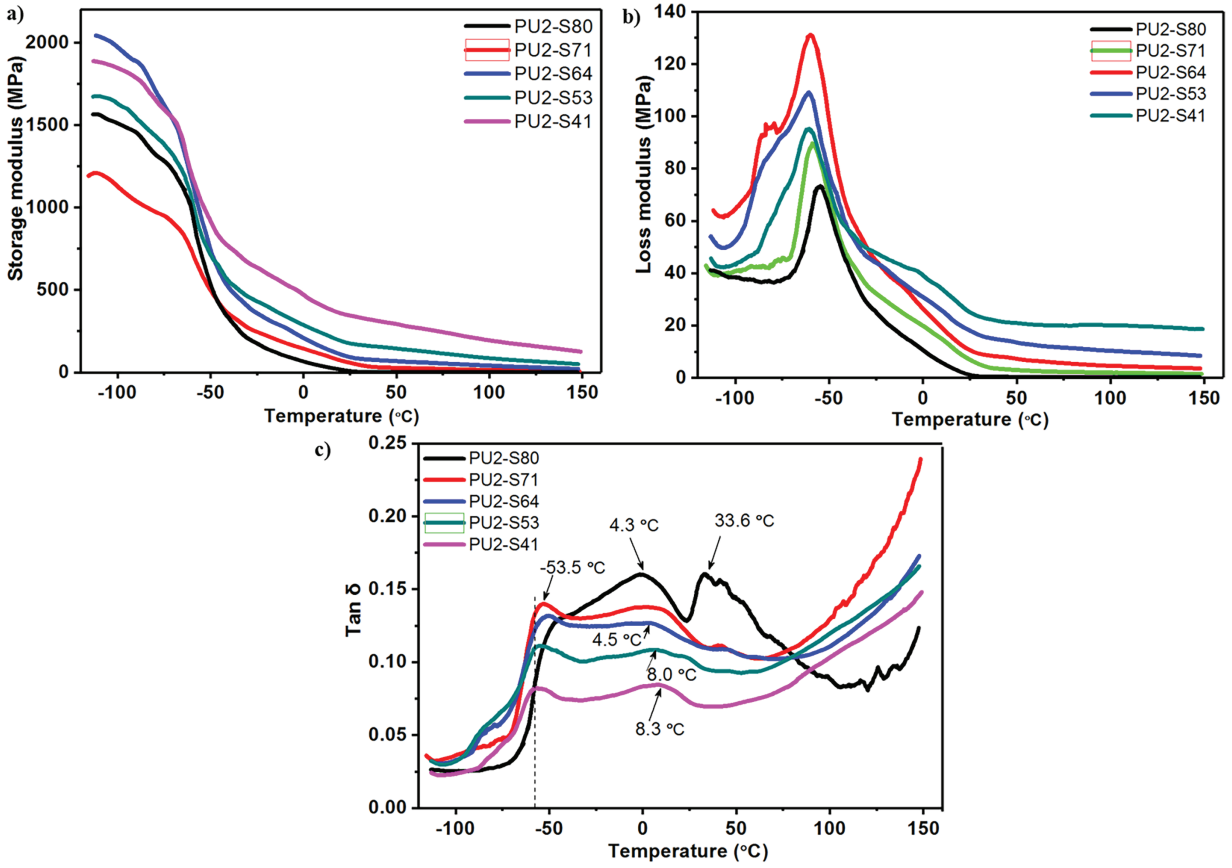

Figure 6: Effect of SS content on (**a**) storage modulus, (**b**) loss modulus and (**c**) loss factor (tan δ) vs. temperature. The dash vertical line in figure (**c**) indicates Tg acquired from DSC

3.3 Effect of Catalyst Concentration

Generally, the catalysts are essential in PU system to promote the reaction between polyether polyol and -NCO, especially for solvent-free PU coatings. To prevent PU coatings from sagging and reduce curing time, solvent-free PU elastomeric coatings should be gelled in a short time, and the organotin catalyst at above 0.1% is usually added into Component B [23]. However, organotin catalyst will also accelerate the reaction rate between H_2O in the atmosphere and -NCO, and further leads to foaming and degradation of the mechanical strength of PU elastomeric coatings. The effect of catalyst on the properties of solvent-free and fast-curing related PU coatings has received little attention in the past.

In the current studies, DB was used as the catalyst, and the DB concentration in Component B was adjusted from 0% to 0.25%. The tensile strength of PU2-C0 (i.e., PU2-S64), PU2-C0.0025, PU2-C0.005, PU2-C0.01, PU2-C0.05 and PU2-C0.25 is 19.9, 31.5, 27.6, 24.1, 23.4 and 12.1 MPa, respectively, and PU2-C0.0025 shows the maximum tensile strength (Fig. 7a). In comparison with PU2-C0, 0.0025% DB increases the tensile strength of coatings from 19.9 to 31.5 MPa. As for the tear strength of PU coatings, PU2-C0.005 is also greatly strengthened by 0.005% DB (Fig. 7b). However, the tensile strength and tear strength are obviously decreased when the DB concentration exceeds 0.005%. The density of the coatings slightly increases from 1.03 to 1.08 g/cm^3 with DB concentration increasing from 0% to 0.005%, but dramatically decreases for further increase of DB concentration (Fig. 7c). The above analysis indicates that DB of extremely low concentration less than 0.005% will promote the curing reaction completely and result in enhancement of mechanical performance. However, the foaming and degradation of the mechanical strength occur when DB concentration exceeds 0.005%. The standard deviation (SD) of tensile strength and elongation at break was investigated to gain a better insight into the effect of the catalyst (Fig. 7d). DB of concentration less than 0.0025% or in excess of 0.05% shows lower SD of tensile strength and elongation at break, while there is a peak of SD at DB concentration between 0.0025% and 0.05%. The above findings indicate that the coatings are homogeneous in structure at DB concentration less than 0.0025% or in excess of 0.05% but asymmetrical in structure at DB concentration between 0.0025% and 0.05%. By combining SD analysis with results of density, it is able to be inferred that the coatings show a high-density uniform structure at DB concentration less than 0.0025%, homogeneous foam structure at DB concentration in excess of 0.05% and foam-hybrid structure at DB concentration of 0.01%. As shown in Fig. 7a,b, the tensile strength indeed decreased from 31.5 to 27.6 MPa when the DB concentration increased from 0.0025% to 0.005%, while the tear strength increased from 77 to 91 N/mm. From this perspective, both 0.0025% and 0.005% DB concentrations perform relatively well. However, as can be seen from Fig. 7d, when the concentration increases to 0.005%, the standard deviations of both tensile strength and elongation at break significantly increase. This indicates a higher probability of internal defects in the samples. Therefore, at a catalyst concentration of 0.0025%, the overall performance is better.

To investigate whether the catalyst content affects the final curing degree of the coatings and further clarify the reasons for the differences in mechanical properties with varying catalyst concentrations, we conducted FTIR analysis (Fig. 8). The peak at 2242 cm^{-1} corresponds to the stretching vibration of -N=C=O in MDI, while the peaks at 3588–3324 and 996 cm^{-1} represent the stretching vibrations of CO-H and C-OH in PTMG, respectively. In the spectrum of PU2-S64, all three characteristic peaks disappear, and a new peak emerges at 1726 cm^{-1}, attributed to the stretching vibration of RNH(C=O)OR. This indicates that in PU2-S64, despite the absence of a catalyst, all -NCO groups in Component A and -OH groups in PTMG from Component B have fully reacted. The FTIR spectra of PU2-C0.0025 to PU2-C0.25 show almost no differences compared to PU2-S64. These results demonstrate that the catalyst content has no significant impact on the final curing extent, and all coatings achieved sufficient curing. However, this does not necessarily imply that the curing degree of PU2-S64 is entirely equivalent to that of PU2-C0.0025. When the curing degree approaches 100%, even minimal differences can lead to substantial variations in the mechanical strength, and such subtle differences are difficult to detect by FTIR. Therefore, we can only infer that the superior

mechanical strength of PU2-C0.0025 compared to PU2-S64 may be attributed to the presence of a catalyst, which potentially facilitates a more complete curing reaction.

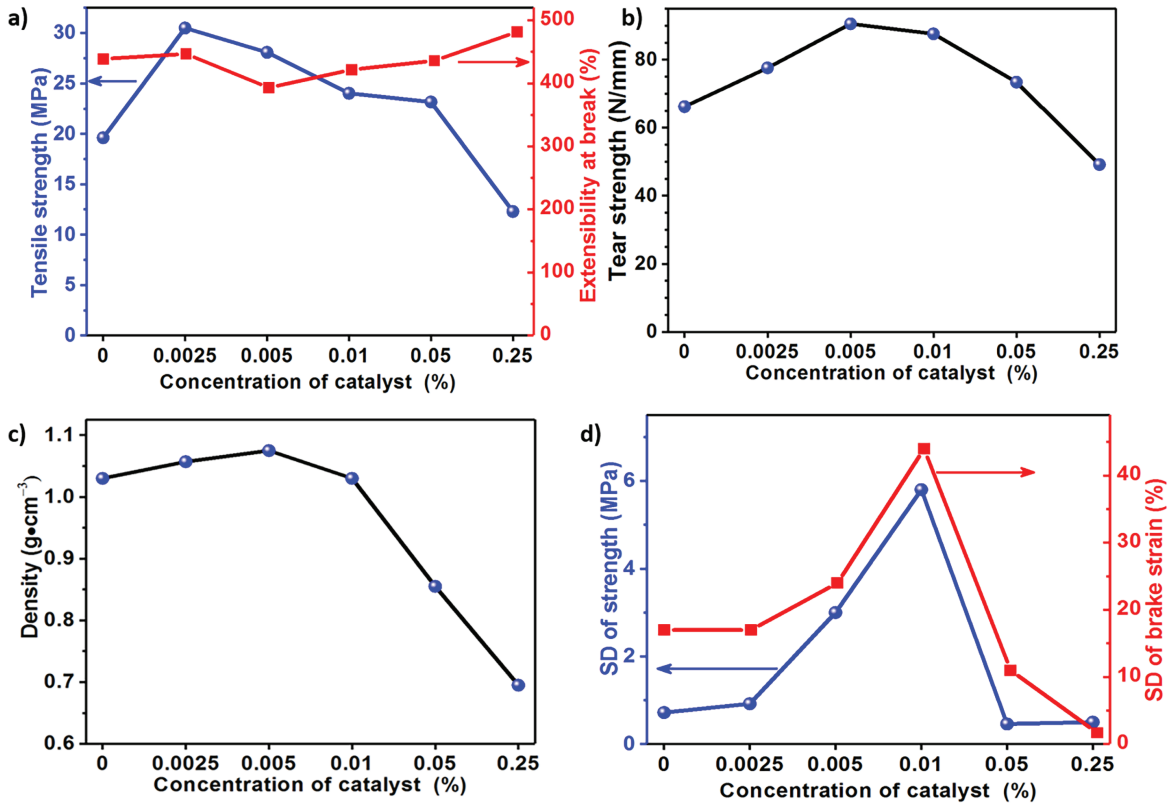

Figure 7: Effect of catalyst concentration on (**a**) tensile strength and extensibility at break, (**b**) tear strength, (**c**) density of coatings and (**d**) mean square deviation of tensile strength and extensibility at break

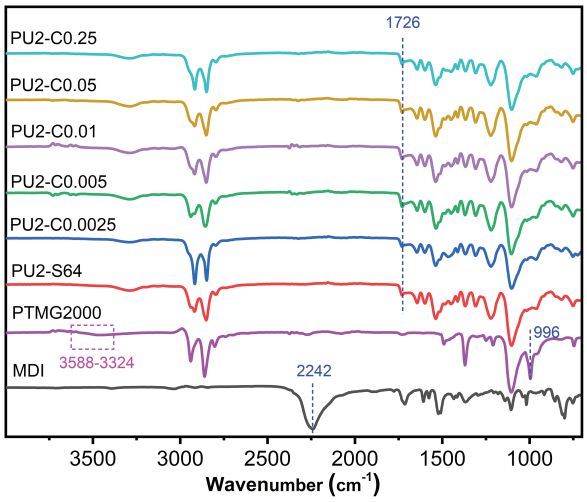

Figure 8: FTIR spectra of coatings with different catalyst contents, including those of MDI and PTMG for reference. The blue dashed lines and purple dashed boxes indicate the main characteristic peaks

The microstructure of PU coatings with different DB concentrations was investigated by SEM (Fig. 9). SEM images show that foam cell sizes of PU2-C0, PU2-C0.0025, PU2-C0.005 range from 20 to 60 μm. The average foam cell size and number of foam cells decrease with an increase in catalyst concentration for PU2-C0, PU2-C0.0025, PU2-C0.005. However, foam cells in excess of 100 μm are observed for PU2-C0.01, and PU2-C0.01 shows a hybrid structure with foam cells of 20–60 μm and foam cells of 140 μm. The number of 100–140 μm foam cells increases as increase of catalyst concentration for PU2-C0.01, PU2-C0.05 and PU2-C0.25. As expected, the microstructure of PU coatings matches the SDs of tensile strength and elongation at break shown in Fig. 7d.

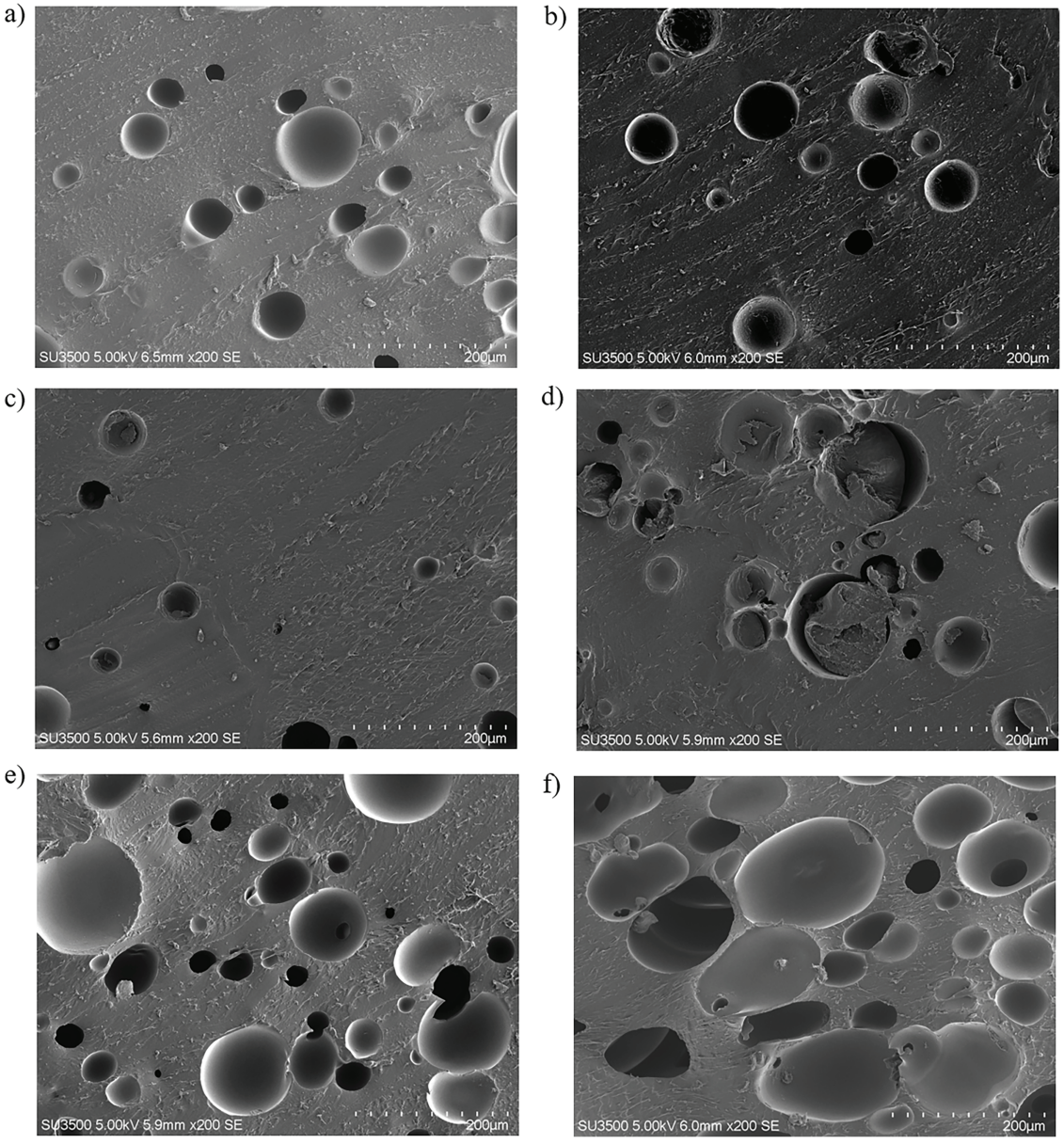

Figure 9: SEM images of PU coatings derived from component B with different DB concentrations, (**a**) PU2-C0, (**b**) PU2-C0.0025, (**c**) PU2-C0.005, (**d**) PU2-C0.01, (**e**) PU2-C0.05 and (**f**) PU2-C0.25

The gel times of PU2-C0, PU2-C0.0025, PU2-C0.005, PU2-C0.01, PU2-C0.05 and PU2-C0.25 are 170, 170, 170, 170, 120 and 60 s, respectively. DB concentration less than 0.01% has no effect on gel time, and the coatings show the same gel time for PU2-C0, PU2-C0.0025, PU2-C0.005 and PU2-C0.01. Gel times of PU2-C0.05 and PU2-C0.25 are dramatically reduced by DB (Fig. 10). By combining the results of mechanical tests with the microstructure of coatings, it can be concluded that DB concentrations below 0.01% in Component B are beneficial for PU elastomeric coatings. A minimum DB concentration of 0.05% is essential to shorten the gel time of coatings to within 2 min, which meanwhile, results in foam and degradation of mechanical strength. Fig. 4c shows gel time of coatings is dramatically affected by the ratio of DMTDA to MDI, so gel time is dominated by not only catalyst, but also chain extender. And it is more practical to adjust the gel time of the coatings by chain extender rather than excess catalyst.

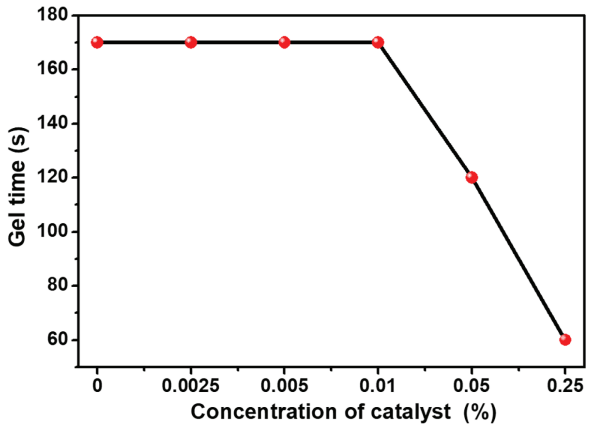

Figure 10: Effect of DB concentration in component B on gel time of the coatings

3.4 Effect of Polyether Polyol Type

The effect of polyether polyol type on the performance of coatings is shown in Table 4. The molecular weight of PTMG in Component A has no effect on the density and gel time of the coatings. As the molecular weight of PTMG in Component A is decreased from 2000 to 1000 g/mol, PU1 presents higher tensile strength, higher peel strength and lower elongation at break (Table 4 and Fig. 11). Compared to PU2-S64C, PU1-S64C exhibits a slight increase in both modulus and toughness, which can be attributed to the smaller molecular weight of PTMG1000, resulting in a shorter distance between the cross-linking points. In contrast, an increase in D2000 content leads to a reduction in modulus, as PTMG2000 is more prone to crystallize. Among the samples, PU2-S64C-D2 demonstrates the highest toughness. Meanwhile, the decrease in molecular weight of PTMG leads to Tg increasing from −53.1°C to −39.4°C, implying PU2-S64C is better in terms of low-temperature performance (Fig. 12).

In addition, part of PTMG in Component B is replaced by D2000 to assess the effect of polyether polyol types on properties of the coatings. Seen from Table 2, the density of coatings decreases from 1.03 to 0.95 g/cm^3 with an increase in D2000 content. The reaction rate between D2000 and -NCO is much faster than that between PTMG and -NCO, which is beneficial for protecting coatings from moisture foaming. However, the increase of D2000 results in dramatic decrease of gel time. It is inevitable that some bubbles are generated by the air flow and sealed into the coatings in the spraying process. These bubbles are fixed into the coatings as a result of dramatic decrease in gel time, and further lead to decrease in coating density. The coating of formulation PU2-S64C-D3 fails to be sprayed because the viscosity increases much faster.

Table 4: Effect of polyether polyol types on the performance of coatings

Serial number	Density, g/cm^3	Gel time, s	Tensile strength, MPa	Elongation at break, %	Tensile modulus, MPa	Toughness, MJ/m^3	Tear strength, N/mm
PU2-S64C	1.03	170	31.3	430	67.8	54.6	66
PU1-S64C	1.03	170	31.0	375	69.7	48.9	74
PU2-S64C-D1	0.96	170	31.2	470	67.3	61.3	74
PU2-S64C-D2	0.95	80	15.4	520	58.4	49.2	69
PU2-S64C-D3	–	50	–	–	–	–	–

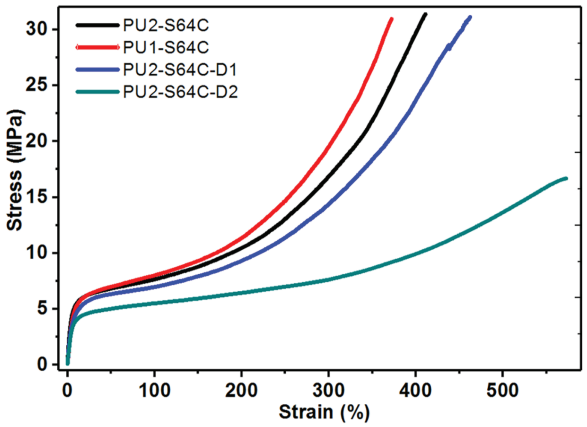

Figure 11: Curves of tensile stress vs. strain for coatings with different polyether polyol types

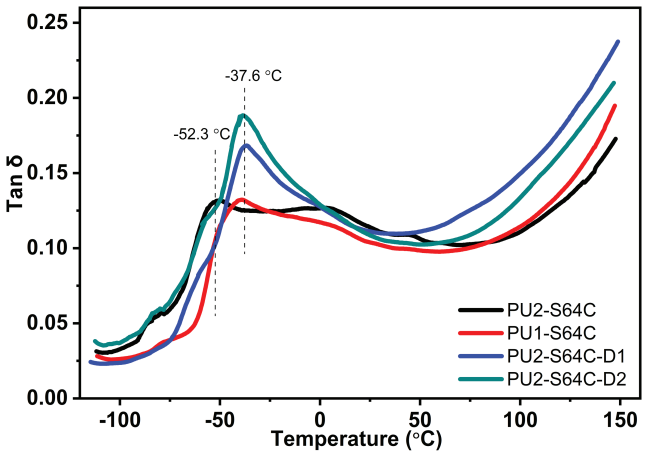

Figure 12: Curves of loss factor (tan δ) against temperature for coatings with different polyether polyol types

PU2-S64C-D1 is roughly equivalent to PU2-S64C in terms of tensile strength and tear strength, indicating a replacement of D2000 for 47% PTMG has little effect on the mechanical strength. However, an obvious decrease of the mechanical strength occurs when 74% of PTMG2000 was replaced by D2000 in Component B (Table 4 and Fig. 11). And Fig. 11 indicates that D2000 dramatically weakens tensile modulus of coatings. As the content of D2000 is increased from 0 g to 166 g, Tg increases from −53.1°C to −36.9°C (Fig. 12).

The above results indicate that PTMG-based PU coatings show superior mechanical properties and low-temperature performance to polyoxypropylene-based PUA coatings, and the coatings derived from PTMG show a tensile strength above 30 MPa and an elongation at break of 400%. To date, it is about 10–20 MPa in terms of tensile strength for PUA coatings with large elongation and elasticity in most reports [24–27]. Although PUA coatings have received phenomenal success in wide applications, the PU coatings in the current research present abundant and large application potential for precision coating and high-tech areas.

4 Conclusion

A series of solvent-free polyurethane elastomeric coatings based on PTMG were successfully prepared via a spray method, demonstrating rapid curing and highly tunable mechanical properties. In the synthesis of Component A, MDI was selected over CMDI due to its lower viscosity, allowing the component to remain applicable at room temperature. Systematic investigation revealed the significant influence of several factors—including SS content, catalyst dosage, polyether molecular weight, and polyether type—on the processing behavior, mechanical performance, morphology, density, and thermal properties of the coatings. Increasing the SS content from 53% to 80% led to a notable rise in breaking elongation from 200% to 650%, along with an increase in SS crystallinity and a reduction in modulus. While the glass transition temperature remained consistently around −60°C with little dependence on SS content, the coating with approximately 64% SS exhibited the highest tensile strength. The gel time and tack-free time were effectively reduced to several minutes through chain-extender optimization rather than merely increasing catalyst content. A catalyst content as low as 0.0025% was sufficient to achieve optimal mechanical properties, whereas exceeding 0.05% caused foaming and a decline in the mechanical strength. Compared to polyoxypropylene diamine, PTMG-based elastomers displayed superior mechanical performance, yielding coatings with tensile strength above 30 MPa and elongation at break exceeding 400%. This work establishes a robust strategy for precision coating of small-scale industrial components, effectively addressing a key limitation in conventional polyurea technologies.

Acknowledgement: Not applicable.

Funding Statement: This research was funded by the National Natural Science Foundation of China (No. U2330207) and the presidential foundation of China Academy of Engineering Physics (No. YZJJZQ2024004).

Author Contributions: The authors confirm contribution to the paper as follows: conceptualization, Zhipeng Ran; methodology, Zhipeng Ran; formal analysis, Zhipeng Ran, Peishuang Xiao; writing—original draft preparation, Zhipeng Ran; writing—review and editing, Zhipeng Ran, Peishuang Xiao, Shuen Liang, Keping Chen, Xiuli Zhao; project administration, Xiuli Zhao; funding acquisition, Xiuli Zhao, Keping Chen. All authors reviewed the results and approved the final version of the manuscript.

Availability of Data and Materials: The data that support the findings of this study are available from the Corresponding Authors upon reasonable request.

Ethics Approval: Not applicable.

Conflicts of Interest: The authors declare no conflicts of interest to report regarding the present study.

References

1. Zhang H, Meng J, Cai L, Wang Z, Tong G. Polyurea: evolution, synthesis, performance, modification, and future directions. Prog Org Coat. 2025;201:109127. doi:10.1016/j.porgcoat.2025.109127.

2. Ding L, Wang Y, Lin J, Ma M, Hu J, Qiu X, et al. Recent advances in polyurea elastomers and their applications in blast protection: a review. J Mater Sci. 2024;59(32):14893–923. doi:10.1007/s10853-024-10050-7.
3. Wang Z, Du M, Fang H, Zhao P, Yao X, Chen S. The development of high-strength, anticorrosive, and strongly adhesive polyaspartate polyurea coating suitable for pipeline spray repairs. J Appl Polym Sci. 2024;141(29):e55668. doi:10.1002/app.55668.
4. Jahan A, Masood S, Zafar F, Rizvi SA, Alam M, Haq QMR, et al. Ambient-cured cardanol-derived polyurea coatings for anti-corrosive and anti-bacterial applications. Prog Org Coat. 2023;182:107638. doi:10.1016/j.porgcoat.2023.107638.
5. Chen D, Wu H, Cheng Y. Dynamic behaviors of unreinforced and spray polyurea retrofitted brick masonry infill walls under blast loads: shock tube test and analyses. Int J Impact Eng. 2024;190:104975. doi:10.1016/j.ijimpeng.2024.104975.
6. Chen D, Wu H, Wei JS, Xu SL, Fang Q. Nonlinear visco-hyperelastic tensile constitutive model of spray polyurea within wide strain-rate range. Int J Impact Eng. 2022;163:104184. doi:10.1016/j.ijimpeng.2022.104184.
7. Wang W, Chen R, Liu P, Liu Q, Liu J, Yu J, et al. Aniline-terminated polyether polyurea with ultra strength, toughness and impact-resistant for enhanced ballistic protection. Prog Org Coat. 2024;189:108249. doi:10.1016/j.porgcoat.2024.108249.
8. Guo H, Sun Y, Xiao Y, Chen Y. Investigation of polyurea coating influence on dynamic mechanical properties of concrete. Structures. 2024;69(7):107446. doi:10.1016/j.istruc.2024.107446.
9. Han X, Hu Y, Ren C, Wang L, Wu L, Sun A, et al. Environmentally friendly fluorine-free anti-fouling polyurea coatings with excellent abrasion resistance. Colloids Surf A Physicochem Eng Asp. 2025;717(41):136751. doi:10.1016/j.colsurfa.2025.136751.
10. Yu Y, Xu L, Liu S, Gu G, Chen Y, Yuan H, et al. Eco-friendly, mechanically robust, weather-resistant and rapidly cured polyurea elastomer synthesized by vat photopolymerization 3D printing. Compos Part A Appl Sci Manuf. 2025;196(1):108985. doi:10.1016/j.compositesa.2025.108985.
11. Lv X, Yan H, Wang Z, Dong J, Liu C, Zhou Y, et al. Effects of hydrogen bonding on photo-responsive behavior of healable azobenzene-containing polyurea elastomers. Opt Mater. 2023;139:113755. doi:10.1016/j.optmat.2023.113755.
12. Zhao YC, Wang XY, Shang K, Zhao B. Solvent-free, slow-curing, and corrosion-resistant flame retardant polyurea enabled by a Schiff base latent curing agent and phosphate polyol. Polym Test. 2025;145:108754. doi:10.1016/j.polymertesting.2025.108754.
13. Iqbal N, Tripathi M, Parthasarathy S, Kumar D, Roy PK. Polyurea spray coatings: tailoring material properties through chemical crosslinking. Prog Org Coat. 2018;123(8):201–8. doi:10.1016/j.porgcoat.2018.07.005.
14. Huang W. Spray polyurea elastomer technology. Chem Ind Press. 2005;4:26. (In Chinese).
15. Chen J, Sun H, Meng Q. Spray polyurethana-urea elastomer prepared by static mixing technology. Mod Coat Finish. 2016;19(12):21–3. (In Chinese).
16. Wu W, Chen F, Diao Z, Xu C, Sun J. Preparation of spray polyurethane-urea elastomer for rubber conveyor belt through static mixing technology. China Coat. 2019;34(10):17–21. (In Chinese). doi:10.1201/9780203740378-16.
17. Van Nguyen T, An Y, Kusano Y, Kageoka M, Feng S, Padermshoke A, et al. Effect of soft segment chemistry on marine-biodegradation of segmented polyurethane elastomers. Polym Degrad Stab. 2025;233:111149. doi:10.1016/j.polymdegradstab.2024.111149.
18. Zhang Z, Yu X, Wang Z, Zhang S, Wang Y, Liu H, et al. MDI-PTMG-based TPU modified asphalt: preparation, rheological properties and molecular dynamics simulation. Fuel. 2025;379(6):133007. doi:10.1016/j.fuel.2024.133007.
19. Sun H, Li F, Wang X, Fu J, Xie Q, Zhou J, et al. Engineering spiro diacetal structure into polyurethane for high toughness and controlled degradation. Mater Today Chem. 2025;46(36):102762. doi:10.1016/j.mtchem.2025.102762.
20. Zhou R, Li W, Li J, Hu J, Gui X, Dong Y, et al. Safety risk investigation of trace moisture on solvent-free polyurethane synthesis reaction. J Ind Eng Chem. 2025;146:357–65. doi:10.1016/j.jiec.2024.11.019.

21. El-Bindary AA, Shoair AF, Kiwaan HA, Eessa AM. Application of vinyltrimethoxy silane as moisture scavenger for the high reactive 2k polyurethane coatings: physicochemical and kinetic studies. J Mol Liq. 2017;244(7):226–32. doi:10.1016/j.molliq.2017.09.013.
22. Holzworth K, Jia Z, Amirkhizi AV, Qiao J, Nemat-Nasser S. Effect of isocyanate content on thermal and mechanical properties of polyurea. Polymer. 2013;54(12):3079–85. doi:10.1016/j.polymer.2013.03.067.
23. Wang N, Wang X, Lang J, Hu Z, Zhang H. Synthesis and characterization of hyperbranched and organosilicone modified waterborne polyurethane acrylates photosensitive resin. Polymers. 2021;13(13):2039. doi:10.3390/polym13132039.
24. Tripathi M, Parthasarathy S, Roy PK. Spray processable polyurea formulations: effect of chain extender length on material properties of polyurea coatings. J Appl Polym Sci. 2020;137(16):48573. doi:10.1002/app.48573.
25. Chen Y, Yang K, Dong H, Niu H, Wang Q, Cheng Q. Synthesis and characterization of silicone polyurea and mechanical properties improvement through interfacial reaction. RSC Adv. 2025;15(15):11835–44. doi:10.1039/d5ra00331h.
26. Iqbal N, Kumar D, Roy PK. Understanding the role of isocyanate dilution toward spraying of polyurea. J Appl Polym Sci. 2018;135(9):45869. doi:10.1002/app.45869.
27. Guo H, Du C, Chen Y, Li D, Hu W, Lv X. Study on protective performance of impact-resistant polyurea and its coated concrete under impact loading. Constr Build Mater. 2022;340(8):127749. doi:10.1016/j.conbuildmat.2022.127749.